Chem. **1998**, *110*, 339 – 343; *Angew. Chem. Int. Ed.* **1998**, *37*, 325 – 329; b) J. J. La Clair, *J. Am. Chem. Soc*. **1997**, *119*, 7676 – 7684.

[8] The photophysics of **1** are further complicated by additional charge transfer states associated with the internal alkyne, see: a) W. Rettig, *Angew. Chem*. **1986**, *98*, 969 – 986; *Angew. Chem. Int. Ed. Engl.* **1986**, *25*, 971 – 988; b) Y. Hirata, T. Okada, T. Nomoto, *Chem. Phys. Lett.* **1997**, *278*, 133 – 138.

[9] LCA is a tetramer composed of two subunits (19874 kDa) of 181 amino acids and two 52 amino acid (5724 kDa) subunits. For crystal structures and sequence information, see: A. Foriers, E. Lebrun, R. Van Rapenbusch, R. de Neve, A. D. Strosberg, *J. Biol. Chem*. **1981**, *256*, 5550 – 5560. Its structure can also be downloaded from the protein databank (PDB) given by 1lem, 1len, 1les, and 2lal.

[10] GNL is a tetramer composed of four identical 109 amino acid (12037 kDa) subunits. For crystal structures and sequence information, see: a) G. Hester, H. Kaku, I. J. Goldstein, C. S. Wright, *Nat. Struct. Biol*. **1995**, *2*, 472 – 479; b) G. Hester, C. S. Wright, *J. Mol. Biol*. **1996**, *262*, 516 – 531; c) G. Hester, C. S. Wright, *Structure* **1996**, *4*, 1339 – 1352. Its structure can also be downloaded from the protein databank given by 1jpc, 1msa, and 1niv.

[11] PSA has a structure comparable to LCA. It is also a tetramer, comprising two 181 amino acid (19969 kDa), and two 52 amino acid (5574 kDa) subunits. For crystal structures and sequence information, see: a) E. J. Meehan, *J. Biol. Chem*. **1982**, *257*, 13278 – 13282; b) G. Gebauer, E. Schilt, H. Rudiger, *Eur. J. Biochem*. **1981**, *113*, 319 – 325. Its structure can also be downloaded from the protein databank given by 1bqp, 1rin, and 2ltn.

[12] Each lectin (GNL, LCA, and PSA) recognizes α-mannopyranosides with affinities ranging from 5 – 100 μM. This includes carbohydrates fused to colorimetric or fluorescent probes through their anomeric center. Typically, the addition of these labels reduces the net affinity of the carbohydrate ligand by an order of magnitude. Based on this assumption, the stoichiometry of lectin to **2** would ensure that at least 80 % of the carbohydrate ligand is bound to the lectin hosts.

[13] Fluorescence measurements were collected on a SLM 8100C Fluorometer equipped with a JD-590 photomultiplier and a 450 W Xenon Arclamp (SLM Instruments).

[14] This difference arose from the structural attributes of these complexes and not from the association or aggregation kinetics of the given complexes. This was verified in that topologies identical to that shown in Figure 2 were also obtained after repeating the measurements after reducing the lectin concentration by 15 %.

[15] BSA does recognize either carbohydrate and therefore serves as a measure of nonspecific interactions. That the fluorescence response from **3** was from nonspecific interactions was further established by comparison with BSA; landscapes generated from addition of **3** either to LCA or BSA were strikingly similar. This result further supports that the fluorescence enhancement with **2** originates, in part, because of docking of the carbohydrate domain in or near the binding pocket of the lectin.

[16] Smoothing was performed using the trinomial algorithm provided within the software package v1995 accompanying the SLM-8100 series 2 spectrometer. The raw data was then processed in Excel97 (Microsoft) and plotted using Origin 5 (Microcal).

Direct Observation of Surface-Controlled Self-Assembly of Coordination Cages by Using AFM as a Molecular Ruler**

Stefano A. Levi, Paolo Guatteri, Frank C. J. M. van Veggel, G. Julius Vancso, Enrico Dalcanale,* and David N. Reinhoudt*

The development of nanotechnology requires miniaturizing complex systems as well as addressing problems at the molecular level.[1] The challenge of overcoming the present limits in routine microfabrication technology in order to reach the nanometer scale requires new methodologies for assembling three-dimensional structures in a controlled fashion directly on solid supports.[2]

In the last few years self-assembly has proven to be a viable alternative to covalent synthesis for the construction of many types of molecular architectures. The desired compounds are formed quantitatively by simply mixing the programmed components under thermodynamic control.[3] Unlike covalent synthesis, self-assembly is a reversible process. This is a very attractive feature because it allows the system to self-repair possible structural deficiencies. Of the self-assembly protocols developed so far, metal-directed self-assembly is particularly appealing as a result of the large number of different structural motifs and bond energies that are available through coordination chemistry.[3a] Until now, the self-assembly approach has mainly been limited to solution chemistry, with very few attempts made to use it directly on surfaces.[4]

Molecular containers represent a very interesting class of compounds[5] as a consequence of their ability to encapsulate ions and neutral molecules. These structures can in principle be addressed individually in a confined environment.[6] Furthermore they are large enough to be detected by scanning force microscopy (SFM).[7] We previously reported the self-assembly of cavitand-based coordination cages formed in solution[8] and the immobilization of covalent container

[*] Prof. Dr. ir. D. N. Reinhoudt, Dr. S. A. Levi, Dr. ir. F. C. J. M. van Veggel
Laboratory of Supramolecular Chemistry and Technology
MESA+ Research Institute, University of Twente
P.O. Box 217, 7500 AE Enschede (The Netherlands)
Fax: (+31) 53-4894645
E-mail: smct@ct.utwente.nl

Dr. E. Dalcanale, Dr. P. Guatteri
Dipartimento di Chimica Organica ed Industriale
Università degli Studi di Parma
Parco Area delle Scienze 17/A, 43100 Parma (Italia)
E-mail: enrico.dalcanale@unipr.it

Prof. G. J. Vancso
Laboratory of Material Science and Polymer Technology
MESA+ Research Institute, University of Twente
P.O. Box 217, 7500 AE Enschede (The Netherlands)

[**] We acknowledge the Nanolink Program of the MESA+ Research Institute (University of Twente), the CNR Nanotechnology Programme, and MURST (Project Molecular Nanoelectronics) for financial support of this work. A special thanks goes to Dr. Maik Liebau (University of Twente) for the preparation of the microcontact-printed substrates and Dr. Frank Geurts (AKZO NOBEL, Central Research Arnhem, NL) for the XPS measurements.

Supporting information for this article is available on the WWW under http://www.angewandte.com or from the author.

  1433-7851/01/4010-1892 $ 17.50+.50/0

molecules on gold.[9] Herein we show a straightforward way to generate coordination cages directly on surfaces by using self-assembled monolayers (SAMs) as molecular platforms. When combined with microcontact-printed (μCP) surfaces this approach allows the direct measurement of the formation of such assemblies on gold without any assumption of parameters.

Monolayers of **1** were prepared by adsorption at 60 °C from a solution of EtOH/$CHCl_3$ (3/1, $c = 0.1$ mM) for at least 12 h.[10] The layers obtained were used to perform the metal-induced capping reactions. Monolayers of cage **6** were assembled by soaking SAMs of **1** in a solution of **2** and **4** in CH_2Cl_2. SAMs of **7** were prepared in the same way using compounds **2** and **5** (Scheme 1).

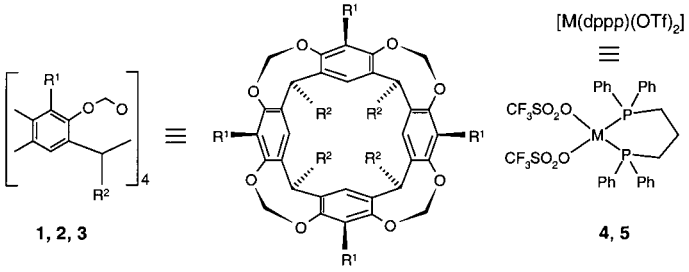

1: R^1 = CN R^2 = $C_{11}H_{22}$-S-$C_{10}H_{21}$
2: R^1 = CN R^2 = C_6H_{13}
3: R^1 = H R^2 = $C_{11}H_{22}$-S-$C_{10}H_{21}$
4: M = Pt
5: M = Pd

Scheme 1. The molecular building blocks: Cavitands **1** and **2** form the upper and the lower halves of the cages, compounds **4** and **5** are the metal complexes which direct the assembly. dppp = 1,3-bis(diphenylphosphanyl)-propane; Tf = F_3CSO_2.

Solution experiments have shown that different R^2 substituents do not bias the outcome of the self-assembly toward the formation of a cage. Under the reported conditions, formation of homocages of **2** occurs in solution, while cages of **6** or **7** form on the surface of the SAM (Scheme 2).

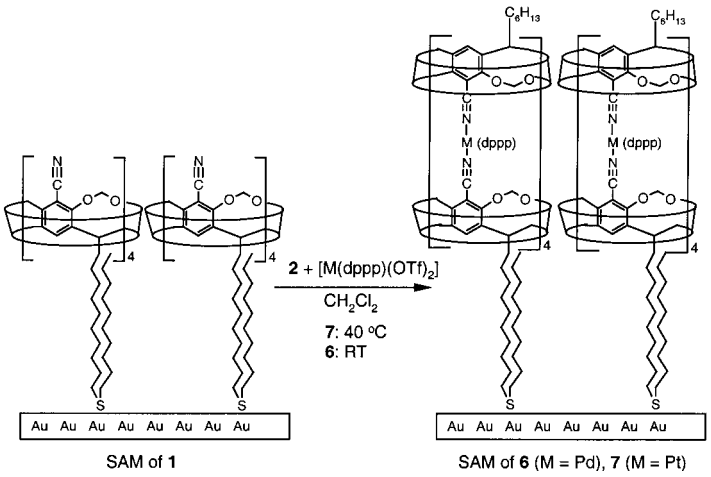

Scheme 2. Representation of the self-assembly reaction that leads to the formation of cages on a SAM.

The formation of cages **6** and **7** on SAMs of **1** was proven by contact-angle measurements, electrochemistry, X-ray photoelectron spectroscopy (XPS), and atomic force microscopy (AFM). The slight variations in the values of the contact angles observed for SAMs of **1**, **6**, and **7**, respectively, indicate that the order of the SAMs after assembly of the cages is maintained (Table 1), which is in accord with previous results from similar monolayers.[9] The value of the capacitance Q_{ml} (ml = monolayer), as measured by cyclic voltammetry (CV),[11] of about 2.3 μF cm^{-2} for monolayers of adsorbate **1** is almost the same as that of well-packed monolayers of equal thickness, such as SAMs of cavitands (1.5–2.5 μF cm^{-2}).[10a]

Table 1. Results obtained from electrochemical and contact-angle measurements.

SAM	Q_{ml}[a] [μF cm^{-2}]	R_{ml}[b] [$10^3\Omega$]	iHET[c] [μA]	Θ_{adv}[d] [°]	Θ_{rec}[d] [°]
1	2.3 ± 0.3	348	0.20 ± 0.05	89 ± 2	50 ± 2
3	2.5 ± 0.3	180	0.50 ± 0.05	105 ± 2	81 ± 2
6	2.0 ± 0.2	634	0.13 ± 0.03	95 ± 2	42 ± 2
7	1.9 ± 0.2	532	0.10 ± 0.03	88 ± 2	53 ± 2

[a] Capacitance of the monolayer measured by cyclic voltammetry (CV) in the absence of a redox couple. [b] Resistance of the monolayer measured by electrochemical impedence spectroscopy (EIS). [c] Heterogeneous electron transfer (HET) measured in the presence of a redox couple. [d] Contact angles (advancing (adv) and receding (rec)) of a water droplet on the monolayer surface.

The respective values of the capacitance decrease after the metal-induced assembly of the cages (Table 1), which indicates there is an increase of the effective thickness (d_{ml})[12] of the SAMs, and is consistent with cage formation on the surface. Heterogeneous electron transfer (HET)[13] and electrochemical impedance spectroscopy (EIS)[14] show a decrease in the intensity of the current and an increase of the resistance in SAMs of **6** and **7**. These data, which are in agreement with the previous results, are consistent with the results found by CV.[15c] In agreement with the electrochemistry results, XPS measurements on SAMs of **6** and **7** reveal the presence of all the elements expected from the molecular structure (Table 2).[15]

A series of control experiments were performed to prove that self-assembly of the cages occurs on the surface of the SAMs through metal coordination. The cage capping on the

Table 2. Results from the XPS elemental analysis.

Peak	SAM of **1**		SAM of **6**		SAM of **7**	
	Measured [%]	Calcd [%]	Measured [%]	Calcd [%]	Measured [%]	Calcd [%]
C-1s	84.4	87.9	74.4	75.2	74.1	75.2
O-1s	11.0	6.1	13.9	10.3	14.4	10.3
N-1s	3.1	3.0	2.6	2.1	2.8	2.1
S-2p	2.3	3.0	4.6	3.1	3.4	3.1
Pd-3d	–	–	n.o.[a]	1.0	–	–
Pt-4f	–	–	–	–	0.5	1.0
P-2p	–	–	2.6	2.1	2.4	2.1
F-1s	–	–	5.1	6.1	4.5	6.1

[a] Values of Pd for cage **6** could not be obtained (n.o.) because of the overlapping proximity of the much more intense Au signal of the substrate.

  1433-7851/01/4010-1893 $ 17.50+.50/0

SAM of cavitand **3** left the monolayer unchanged, as proven by electrochemistry measurements; this occurs since **3** cannot coordinate metals because it lacks nitrile functionalities. A second control experiment consisted of the treatment of the SAM of **6** with triethylamine, which is able to shift the equilibrium towards the formation of $[M(dppp)(NEt_3)_2](OTf)_2$ plus cavitand **1**.[8] The complete disassembly of the cages on the SAM was monitored by electrochemistry, and the results were in full agreement with the expectations (Table 3).

Table 3. Electrochemical analyses of control experiments.[a]

SAM	Q_{ml} [$\mu F\,cm^{-2}$]	*i*HET [μA]	R_{ml} [$10^3\Omega$]
3	2.5 ± 0.20	0.50 ± 0.05	180
3+metal complex	2.8 ± 0.20	0.53 ± 0.05	150
6	2.1 ± 0.20	0.08 ± 0.02	650
6+Et_3N	2.3 ± 0.20	0.17 ± 0.02	350

[a] See the footnotes in Table 1 for an explanation of the represented quantities.

The formation of the molecular cages was monitored directly by atomic force microscopy (AFM). For this purpose microcontact-printed templates were created using standard soft lithography methods.[16] These templates showed the presence of very regular features over large areas (Figure 1). By means of wet-etching,[16] grooves exposing bare gold were formed with an arbitrary depth (6.9 nm).[17] In this way we obtained a sample in which stripes with a lower height correspond to areas of bare gold, and stripes with a higher topographic profile which are covered by the SAM of 11-sulfanylundecanol.[18] After deposition of a monolayer of cavitand **1** on the bare gold grooves, AFM was used to directly measure changes in the depth of the modified grooves (4.3 nm). The height difference of 2.6 nm (Figure 1 A and B) is consistent with the formation of a monolayer of **1**. Formation of the molecular cages on the printed layers was performed using the same procedure as for the full monolayers. A total difference of 4.2 nm was measured after assembly of the cages (Figure 1 C), a value which is consistent with the calculated dimensions of the assembly. The self-assembly of the cages was monitored by comparing the relative height differences.

The attractiveness of this very simple method is the possibility to track changes at a nanometer level directly.[19] Unlike other techniques that measure thickness (for example, ellipsometry, electrochemistry), AFM does not make use of parameters (for example, dielectric constant, refractive index of the SAM) that are approximations because of the difficulty of measuring them. The presence of an internal fixed height reference—namely, the grooves in the microcontact-printed substrates—allows statistical analysis to be performed on thickness variations of the adsorbed organic layer. All heights recorded by AFM were plotted against the *z*-axis and showed that the measured heights follow a Gaussian distribution, thus allowing an estimation of the statistical error.[20] In this way AFM can be used as a "molecular ruler" to measure the thickness of monolayers.[21]

The insertion of sulfides into SAMs of thiols has been recently investigated in our group.[22] We prepared a SAM where single cavitands could be detected far apart from each other by AFM to study the formation of the coordination cages individually. Insertion of cavitand **1** into a monolayer of sulfanylundecanol was achieved by soaking SAMs of thiol into a 0.1 mM solution of **1** in ethanol for one hour. Under these experimental conditions an average of 20 – 25 molecules per μm^2 were inserted into the SAM.[23] Extensive washing with large amounts of solvents ensured the removal of all physisorbed material. AFM experiments and profile analysis showed the presence of individual round entities which were protruding from the flat monolayer.[24] A height profile analysis revealed that these entities all had the expected size of approximately 2 nm.[25] The formation of the cages **6** and **7** by the addition of **2** and **4** or **5**, respectively, was performed on these samples as described above for the full monolayers. AFM analysis on the new samples revealed the presence of two different types of features: 1) individual dots with heights

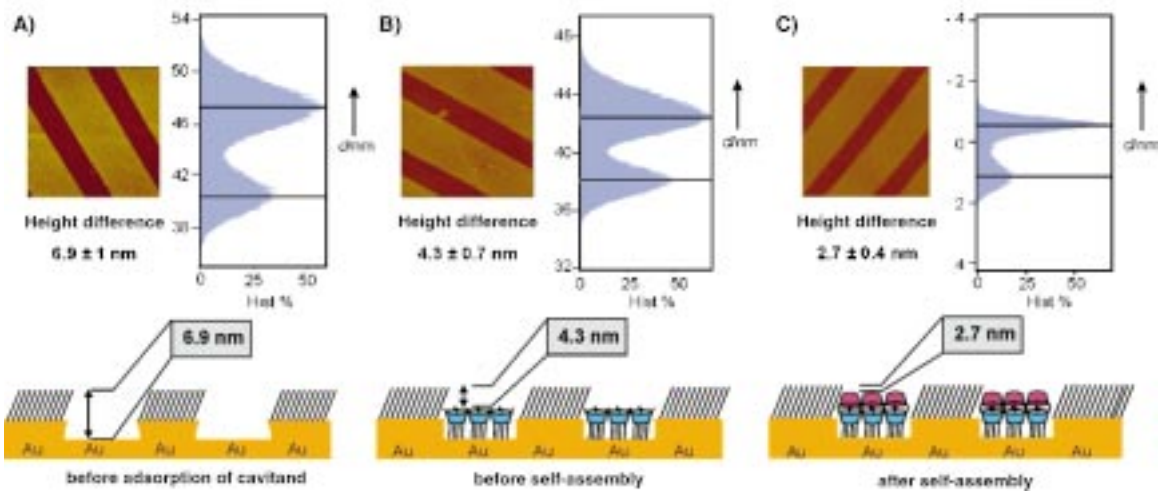

Figure 1. Self-assembly of coordination cages on μ-CP-modified substrates. The grooves on the substrates were obtained by first printing and subsequently wet-etching procedures. The AFM picture, the corresponding histogram, and a schematic representation of the surface is shown for each.

  1433-7851/01/4010-1894 $ 17.50+.50/0 *Angew. Chem. Int. Ed.* **2001**, *40*, No. 10

of about 4 nm and 2) individual dots with heights of about 2 nm (Figure 2). We attribute the two different entities to the two different species: the cavitand and the coordination cages adsorbed on the Au surface.[26]

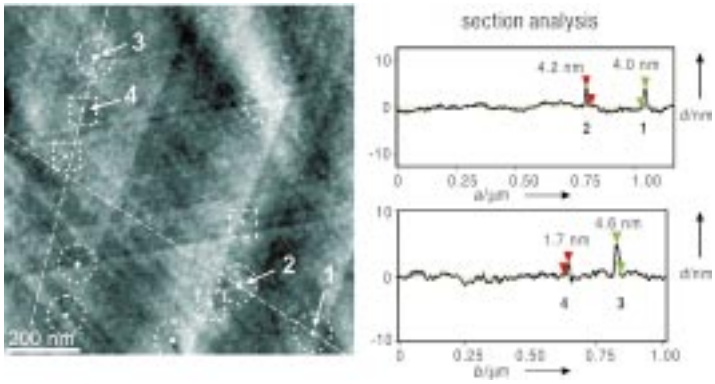

Figure 2. AFM image and height profiles of individual cages along slices *a* and *b*. Annealing the gold substrate before SAM deposition provided atomically flat terraces. Lower objects (dotted squares) are attributed to the residual cavitand **1** molecules, while higher objects (dotted circles) correspond to single cages **6**.

In summary, we have observed directly the self-assembly of coordination cages directly on SAMs on gold surfaces. The self-assembly process was monitored by directly measuring the height profile of these cages by means of AFM using substrates containing internal height references prepared by microcontact printing. We performed and monitored the formation of the assembly on a single molecular level, where we observed both cavitands and cages formed by metal-induced coordination.

Experimental Section

Cavitand **1** was prepared from the corresponding tetrabromo derivative.[27] All monolayers were prepared using standard procedures.[28] The gold substrates were cleaned in oxygen plasma and immersed for 10 minutes in pure ethanol before use.[29] Microcontact-printed substrates were prepared by standard lithography techniques.[16] Electrochemical experiments were performed according to literature procedures[30] and spectra were analyzed by using the software package "Equivalent Circuit".[31] Detailed descriptions of the experimental procedures can be found in the Supporting Information.

Received: December 20, 2000 [Z16310]

[1] C. P. Collier, G. Mattersteig, E. W. Wong, Y. Luo, K. Beverly, J. Sampaio, F. M. Raymo, J. F. Stoddart, J. R. Heath, *Science* **2000**, *289*, 1172 – 1175.

[2] *Nanotechnology, Towards a Molecular Construction Kit* (Ed.: A. ten Wolde), Netherlands Study Center for Technology Trends, The Hague, **1998**, pp. 225 – 229.

[3] a) S. Leininger, B. Olenyuk, P. J. Stang, *Chem. Rev.* **2000**, *100*, 853 – 908; b) M. M. Conn, J. Rebek, Jr., *Chem. Rev.* **1997**, *97*, 1647 – 1668.

[4] a) I. Weissbuch, P. N. W. Baxter, S. Cohen, H. Cohen, K. Kjaer, P. B. Howes, J. Als-Nielsen, G. S. Hanan, U. S. Schubert, J.-M. Lehn, L. Leiserowitz, M. Lahav, *J. Am. Chem. Soc.* **1998**, *120*, 4850 – 4860; b) A. Hatzor, T. Moav, H. Cohen, S. Matlis, J. Libman, A. Vaskevich, A. Shanzer, I. Rubinstein, *J. Am. Chem. Soc.* **1998**, *120*, 13469 – 13477; c) A. Hatzor, T. van der Boom-Moav, S. Yochelis, A. Vaskevich, A. Shanzer, I. Rubinstein, *Langmuir* **2000**, *16*, 4420 – 4423.

[5] a) D. J. Cram, J. M. Cram, *Container Molecules and Their Guests*, Royal Society of Chemistry, Cambridge, **1994**, p. 4; b) A. Jasat, J. C. Sherman, *Chem. Rev.* **1999**, *99*, 931 – 967; c) T. Kusukawa, M. Fujita, *Angew. Chem.* **1998**, *110*, 3327 – 3329; *Angew. Chem. Int. Ed.* **1998**, *37*, 3142 – 3144; d) T. Kusukawa, M. Fujita, *J. Am. Chem. Soc.* **1999**, *121*, 1397 – 1398.

[6] a) A. J. Parola, F. Pina, E. Ferreira, M. Maestri, V. Balzani, *J. Am. Chem. Soc.* **1996**, *118*, 11610 – 11616; b) S. Mendoza, P. D. Davidov, A. E. Kaifer, *Chem. Eur. J.* **1998**, 4, 864 – 870.

[7] B.-H. Huisman, D. M. Rudkevich, A. Farran, W. Verboom F. C. J. M. van Veggel, D. N. Reinhoudt, *Eur. J. Org. Chem.* **2000**, 269 – 274.

[8] P. Jacopozzi, E. Dalcanale, *Angew. Chem.* **1997**, *109*, 665 – 667; *Angew. Chem. Int. Ed. Engl.* **1997**, *36*, 613 – 615.

[9] B.-H. Huisman, D. M. Rudkevich, F. C. J. M. van Veggel, D. N. Reinhoudt, *J. Am. Chem. Soc.* **1996**, *118*, 3523 – 3524.

[10] a) E. U. Thoden van Velzen, J. F. J. Engbersen, P. J. de Lange, J. W. Mahy, D. N. Reinhoudt, *J. Am. Chem. Soc.* **1995**, *117*, 6853 – 6862; b) B.-H. Huisman, E. U. Thoden van Velzen, F. C. J. M. van Veggel, J. F. J. Engbersen, D. N. Reinhoudt, *Tetrahedron Lett.* **1995**, *36*, 3273 – 3276.

[11] H. O. Finlkea, A. J. Bard, I. Rubinstein, *Electroanalytical Chemistry, Vol. 19*, Marcel Dekker, New York, **1996**, pp. 109 – 355.

[12] The effective thickness of the monolayer d_{ml} [Å] can, in principle, be calculated from $d_{eff} = \varepsilon_0 \varepsilon_{rel}/C_{ml}$ where ε_0 is the permittivity of vacuum (8.9×10^{-12} F m^{-1}) and ε_{rel} is the relative permittivity; however, the value of ε_{rel} is unknown and may vary between 2 and 10 depending on the polarity of the SAM.

[13] K. Takehara, H. Takemura, *Bull. Chem. Soc. Jpn.* **1995**, *68*, 1289 – 1296.

[14] a) R. P. Janek, W. R. Fawcett, A. Ulman, *J. Phys. Chem. B* **1997**, *101*, 8550 – 8558; b) R. P. Janek, W. R. Fawcett, A. Ulman, *Langmuir* **1998**, *14*, 3011 – 3018.

[15] a) E. B. Troughton, C. D. Bain, G. M. Whitesides, R. G. Nuzzo, D. L. Allara, M. D. Porter, *Langmuir* **1998**, *4*, 365 – 385; b) T. Moav, A. Hatzor, H. Cohen, J. Libman, I. Rubinstein, A. Shanzer, *Chem. Eur. J.* **1998**, *4*, 502 – 507; c) M. W. J. Beulen, J. Bügler, B. Lammerink, F. A. J. Geurts, E. M. E. F. Biemond, K. G. C. van Leerdam, F. C. J. M. van Veggel, J. F. J. Engbersen, D. N. Reinhoudt, *Langmuir* **1998**, *14*, 6424 – 6429.

[16] Y. Xia, G. M. Whitesides, *Angew. Chem.* **1998**, *110*, 568 – 594; *Angew. Chem. Int. Ed.* **1998**, *37*, 550 – 575, and references therein.

[17] The standard deviation σ of the measured values was calculated using the height at 68% of the Gaussian distribution histograms.

[18] The roughness of the Au surface (2 nm) measured by AFM did not vary upon exposure to the etchant.

[19] The piezo-scanner of the AFM was calibrated using annealed gold substrates as a reference. By measuring the monoatomic steps on the gold surfaces it was possible to determine the accuracy of the calibration and correct for it. An average value of 2.9 Å was calculated after measuring steps formed by 5 or 6 atomic layers. The standard deviation was found to be within 10%.

[20] A series of control experiments were performed to study the dependency of the height signal obtained by AFM on varying the scanning conditions and by using different cantilevers. Variations of less than 5% of the measured height were observed for all used cantilevers on increasing the force twofold.

[21] A direct comparison between the SAMs adsorbed on the grooves and the printed alkylthiols is possible because there are no edge effects and because the roughness of the two surfaces stays the same.

[22] A. Friggeri, H. Schönherr, H.-J. van Manen, B.-H. Huisman, G. J. Vancso, J. Huskens, F. C. J. M. van Veggel, D. N. Reinhoudt, *Langmuir* **2000**, *16*, 7757 – 7763.

[23] By increasing the soaking time the number of adsorbed molecules increases.

[24] At this stage the AFM measurements do not allow the determination as to whether all four sulfides are coordinated to the gold.

[25] All the individual cavitands measured showed a slightly lower height as a result of the cavitand molecules being inserted into an 8-Å-thick monolayer of thiols.

[26] From the measured sample it appears that only 50% of the cavitand undergoes the capping reaction. This is not surprising considering that the very dilute conditions exclude the cooperativity factor, which is important in self-assembly processes.

  1433-7851/01/4010-1895 $ 17.50+.50/0

[27] a) See the Supporting Information for a complete description of the synthesis and the analytical data; b) E. U. Thoden van Velzen, Ph.D. Thesis, University of Twente, The Netherlands, **1994**.
[28] a) D. A. Dobbs, R. G. Bergman, K. H. Theopold, *Chem. Eng. News* **1990**, *68*(17), 2; b) T. Wnuk, *Chem. Eng. News* **1990**, *68*(26), 2; c) S. L. Matlow, *Chem. Eng. News* **1990**, *68*(30), 2.
[29] H. Ron, I. Rubinstein, *Langmuir* **1994**, *10*, 4566 – 4573.
[30] a) See the Supporting Information for the complete experimental details; b) M. W. J. Beulen, M. I. Kastenberg, F. C. J. M. van Veggel, D. N. Reinhoudt, *Langmuir* **1998**, *14*, 7463 – 7467.
[31] a) B. A. Boukamp, *Equivalent Circuit*, *version 4.55*, University of Twente, Department of Chemical Technology, Enschede, The Netherlands, **1996**; b) B. A. Boukamp, *Solid State Ionics* **1986**, *18 – 19*, 136 – 140; c) B. A. Boukamp, *Solid State Ionics* **1986**, *20*, 31 – 44.

Highly Enantioselective Allylation of Imines with a Chiral Zirconium Catalyst**

Thomas Gastner, Haruro Ishitani, Ryo Akiyama, and Shū Kobayashi*

Over the past several years, powerful asymmetric catalytic variants for many basic synthetic reactions have been developed,[1] and in this large and fast-expanding area of chemistry, several chiral Lewis acids have been successfully used as catalysts.[2] Although highly effective methods that follow this approach for the catalytic asymmetric alkylation of carbonyl compounds have been reported,[3] only very few examples are known for their aza analogues.[4] In the case of imines, the Lewis acids are often deactivated or decomposed by the nitrogen atoms of the starting materials or products, and therefore, catalytic reactions are difficult to perform.

The synthesis of chiral homoallylic amines is of particular interest since they can be used as versatile synthetic intermediates and can be easily converted into many different functional groups.[5] The first catalytic asymmetric allylation of imines was reported in 1998 by Yamamoto and co-workers using allyltributylstannane in the presence of a chiral π-allylpalladium complex.[6] In 1999, Jørgensen and co-workers reported the catalytic asymmetric allylation of α-imino esters.[7] In recent reports, we have demonstrated the extraordinary potential of zirconium(IV) as a metal center for the design of chiral Lewis acid catalysts that are suitable for the activation of bidentate imino compounds in an efficient way.[8]

[*] Prof. Dr. S. Kobayashi, Dr. T. Gastner, Dr. H. Ishitani, R. Akiyama
Graduate School of Pharmaceutical Sciences
The University of Tokyo
CREST, Japan Science and Technology Corporation (JST)
Hongo, Bunkyo-ku, Tokyo 113-0033 (Japan)
Fax: (+81) 3-5684-0634
E-mail: skobayas@mol.f.u-tokyo.ac.jp

[**] This work was partially supported by a Grant-in-Aid for Scientific Research from the Ministry of Education, Science, Sports, and Culture, Japan. The authors are grateful to Dr. Motoo Shiro (Rigaku Co. Ltd.) for his help in performng the X-ray analysis of compound **3cd**. T.G. thanks the Japan Society for the Promotion of Science (JSPS) for the award of a postdoctoral research fellowship.

Supporting information for this article is available on the WWW under http://www.angewandte.com or from the author.

In this paper, the viability of this approach is illustrated by the allylation of imines **1** with allylstannanes **2** to afford the corresponding homoallylic amines **3** in good yields and with high stereoselectivities (Scheme 1).

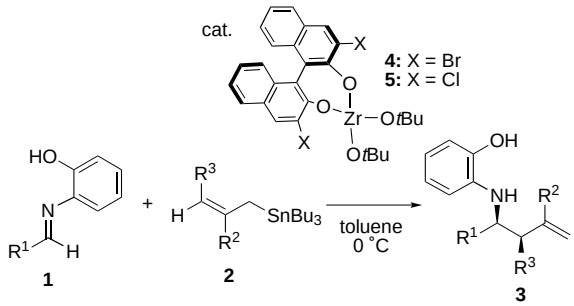

1a: R^1 = Ph
1b: R^1 = 1-naphthyl
1c: R^1 = 3,4-$(OCH_2O)C_6H_3$
1d: R^1 = 2,3-$(MeO)_2C_6H_3$
1e: R^1 = 2-furyl
1f: R^1 = *p*-ClC_6H_4

2a: R^2 = CH_3, R^3 = H
2b: R^2 = CH_2OTBS, R^3 = H
2c: R^2 = CH_2OH, R^3 = H
2d: R^2 = CH_2OH, R^3 = CH_3

Scheme 1. Catalytic asymmetric allylation of imines. TBS = *tert*-butyldimethylsilyl.

We first screened different BINOL derivatives and additives, and found that preparation of the catalyst in situ from $Zr(OtBu)_4$ and an equimolar amount of (*R*)-3,3′-dibromo-1,1′-bi-2-naphthol ((*R*)-3,3′-Br_2BINOL) or (*R*)-3,3′-dichloro-1,1′-bi-2-naphthol ((*R*)-3,3′-Cl_2BINOL) in toluene gave the best results.[9] Conversion of imine **1a** was carried out with stannanes **2a – c** (Table 1). The use of **2a** and **2b** resulted in modest enantioselectivities,[10] and reaction times up to 30 hours were required. A remarkable acceleration of the reaction rate and improved enantioselectivities were observed with stannane **2c** in which the alcohol functionality is unprotected.[10] The reaction was completed within 2 hours, and an 86% yield and an enantiomeric excess of 83% were obtained. In an attempt to extend the scope of this reaction, allylstannane **2d**, with a methyl substituent at the C-3 position, has also been studied.[11] As can be seen from Table 2, improved enantioselectivities and excellent *syn*/*anti* ratios were obtained. The absolute configuration of **3cd** (R^1 = 3,4-$(OCH_2O)C_6H_3$, R^2 = CH_2OH, R^3 = CH_3) was determined to be 3*R*,4*S* by X-ray crystal structure analysis.[12] Interestingly, nearly identical yields and asymmetric inductions were observed with catalysts **4** and **5**. However, catalyst **5**

Table 1. Enantioselective allylation of imines with allylstannanes **2a – c**[a].

Entry	Imine	Stannane	Yield [%]	*ee* [%]
1	**1a**	**2a**	74	55
2	**1a**	**2b**	74	54
3	**1a**	**2c**	86	83
4	**1b**	**2c**	91	68

[a] 10 mol% of catalyst **4** was used.

  1433-7851/01/4010-1896 $ 17.50+.50/0